molecular pharmaceutics

ARTICLE

pubs.acs.org/molecularpharmaceutics

Ion-Activated *In Situ* Gelling Systems for Antisense Oligodeoxynucleotide Delivery to the Ocular Surface

Ilva D. Rupenthal,*[,†] Raid G. Alany,[‡,§] and Colin R. Green[†]

[†]Department of Ophthalmology, Faculty of Medical and Health Sciences and [‡]Drug Delivery Research Unit, School of Pharmacy, Faculty of Medical and Health Sciences, The University of Auckland, Private Bag 92019, Auckland 1142, New Zealand

[§]School of Pharmacy and Chemistry, Kingston University London, Kingston upon Thames, Surrey, U.K.

ABSTRACT:

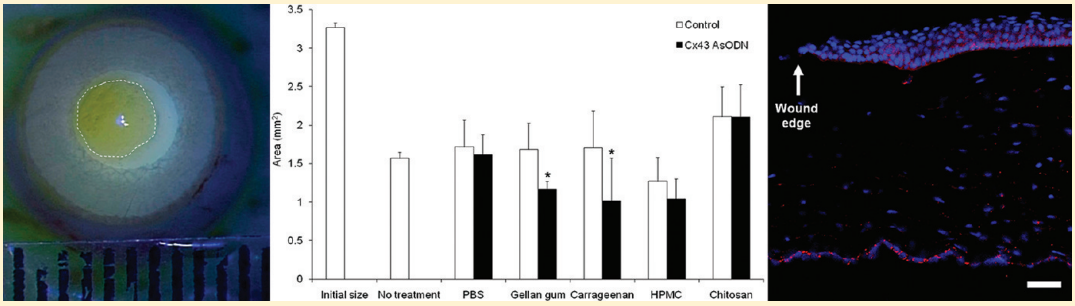

Ion-activated *in situ* gelling systems are able to cross-link with the cations present in the tear fluid, forming a gel on the ocular surface and prolonging corneal contact time. Corneal scrape wounding offers an exceptional model to investigate the efficacy of these formulations for connexin43 (Cx43) antisense oligodeoxynucleotide (AsODN) delivery used to improve wound repair. Systems based on gellan gum and carrageenan have previously been found advantageous in terms of their physicochemical properties, *in vitro* and *in vivo* release profiles and precorneal retention. The present study describes AsODN penetration into corneal tissue after wounding and determines the formulations' delivery efficacy by evaluating wound size, tissue inflammation and connexin levels. No difference was shown between the penetration patterns of the formulations, with most of the AsODN accumulating in the epithelium close to the wound leading edge and the stroma underlying the wound. However, significant differences were seen in the delivery efficacy, with gellan gum and carrageenan based systems resulting in the lowest connexin levels and subsequently in the greatest reduction in wound size, the least stromal edema and hypercellularity. This demonstrates their potential use as delivery vehicles for AsODNs to the ocular surface.

KEYWORDS: wound healing, antisense, ocular drug delivery, *in situ* gelling systems, immunohistochemistry, confocal microscopy

INTRODUCTION

Laser ablation of the cornea to correct refractive errors has become a routine procedure for the ophthalmologist. However, clinical outcomes can be variable depending on the patient's age and condition, the degree of correction and the procedure selected. A number of common complications, such as over-correction, undercorrection, regression and haze, are directly related to the healing process and the unpredictable nature of the associated corneal cellular responses.[1] Epithelial injury initiates a complex sequence of events mediated by cytokines, growth factors and chemokines (Figure 1), and a number of studies have investigated the mechanisms underlying corneal wound healing in an attempt to modulate the healing response.[2−5] Besides the components of the wound healing cascade, gap junctions formed by connexin proteins[6−9] are thought to play a major role during tissue injury and repair.[10−15]

Connexin43 (Cx43) is the most ubiquitous connexin in the cornea. Beyer et al.[16,17] were the first to describe Cx43 in corneal fibroblasts and documented its predominant expression in the basal cells of the corneal epithelium. Ratkay-Traub et al.[18] investigated the changes in Cx43 expression following excimer laser photorefractive keratectomy in rabbits and reported Cx43 levels to be upregulated and its expression to be relocated to the upper cell layers of the epithelium 24 h after surgery. Recent work by Laux-Fenton[10] further examined Cx43 dynamics during normal corneal wound healing using a rat scrape wound model as well as excimer laser surgery and found Cx43 downregulation in the migrating epithelium at the wound front, but upregulation in the dividing epithelium further back from the wound leading edges. Cx43 was also upregulated in the stroma, where it was associated with corneal haze and hypercellularity.

Using an antisense approach to knockdown Cx43 has previously been reported to improve the healing of skin incision, excision and burn wounds.[11,12] Initial studies applying Cx43 antisense oligodeoxynucleotides (AsODNs) to the corneal surface resulted in transient downregulation of Cx43 protein levels at the wound site, which dramatically increased the rate of wound

Received: March 19, 2011
Accepted: October 9, 2011
Revised: September 5, 2011
Published: October 09, 2011

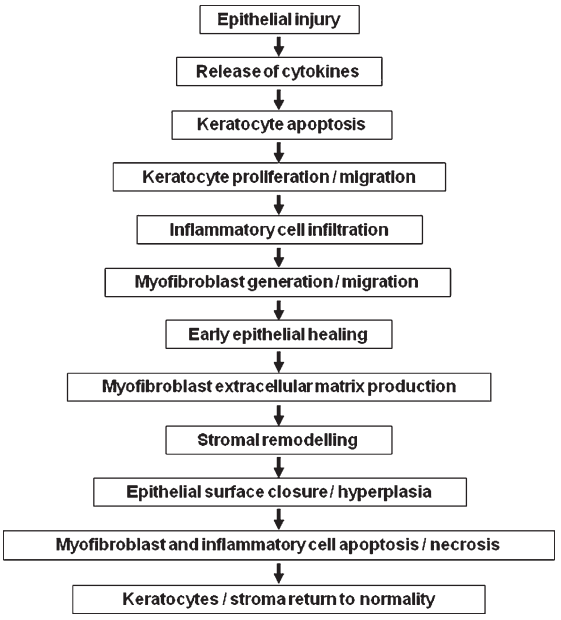

Figure 1. The corneal wound healing cascade.

closure.[10] Lower Cx43 levels were associated with a reduced activation of myofibroblasts, which normally occurs after wounding[19−21] and is thought to be responsible for corneal haze.[22,23] Moreover, reduction in Cx43 levels resulted in earlier epithelial cell movement, reduced hypercellularity at the wound site 24 to 48 h after surgery, inhibited stromal edema and cell proliferation, reduced epithelial hyperplasia and a more regular epithelial−stromal adhesion matrix.[10] That study used a subconjunctival injection of a 30% (w/v) Pluronic F-127 gel, which is an invasive procedure that can result in bleeding at the site of injection, directly affecting the integrity of the AsODNs due to the serum nuclease present in the blood.[24,25] Moreover, Pluronic gel has some drawbacks as it must be kept refrigerated and rapidly gels at room temperature, forming a thick gel mass on the ocular surface. This may induce reflex blinking and disturb vision.

Ion-activated *in situ* gelling systems on the other hand are able to cross-link with the cations present in the tear fluid to form a homogeneous gel on the ocular surface. These gels have been shown to prolong the precorneal retention time and therefore lead to increased bioavailability of model hydrophilic drugs.[26−31] The rapid turnover rate of the lacrimal fluid, which normally leads to a dilution of common viscous eye drops, may for ion-activated gels result in increased viscosity with the increasing amount of cations present.[32] Ion-activated *in situ* gelling systems based on gellan gum and carrageenan have previously been evaluated for ocular use in terms of their physicochemical characteristics, *in vitro* and *in vivo* release profiles and precorneal retention behavior and were found advantageous over formulations based on neutrally charged HPMC, positively charged chitosan or saline alone.[33,34] The present study assessed their efficacy to successfully deliver Cx43 AsODNs to the wounded ocular surface using a rat corneal scrape model. AsODN penetration depth into the corneal tissues was determined 3 h after corneal wounding using confocal laser scanning microscopy. The reduction in wound size of untreated and treated corneas was measured 12 h after scrape wounding using fluorescein staining. The histology of the corneas was compared in terms of stromal thickness and cell infiltration into the stroma, and Cx43 levels were assessed using immunohistochemistry.

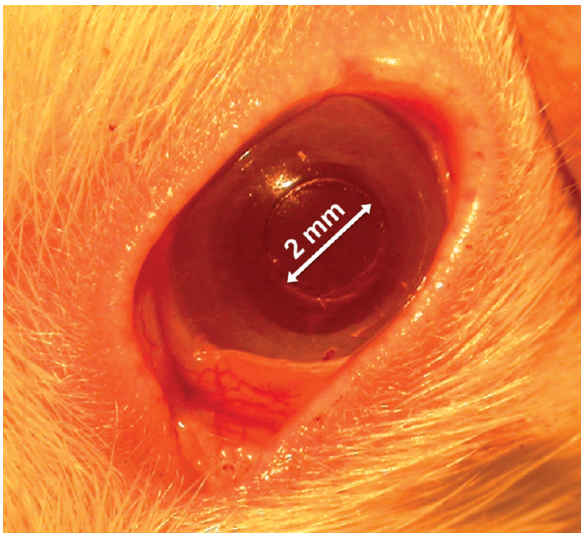

Figure 2. Rat eye showing the demarcated wound area after removal of the corneal epithelium.

MATERIALS AND METHODS

Materials. Gellan gum (Kelcogel F) and carrageenan (Genulacta L-100) were a generous gift from CP Kelco (Atlanta, GA, USA). Hydroxypropyl methylcellulose (HPMC, Methocel K4M) was purchased from Colorcon (Gao, India), while chitosan (Protasan UP CL 213) was obtained from Novamatrix (Sanvika, Norway). Unmodified mouse anti-Cx43 ODNs (5′-GTA-ATT-GCG-GCA-GGA-GGA-ATT-GTT-TCT-GTC-3′) and Cy3-tagged mouse anti-Cx43 ODNs (5′-Cy3-GTA-ATT-GCG-GCA-GGA-GGA-ATT-GTT-TCT-GTC-3′) were purchased from Sigma Genosys (Sigma-Aldrich, Castle Hill, NSW, Australia). The monoclonal rabbit anti-Cx43 primary antibody was from Sigma Chemical Co. (Sigma, Saint Louis, MO, USA), while the Cy3-conjugated affinity purified goat anti-rabbit IgG (H+L) secondary antibody was supplied by Jackson Immuno Research (West Grove, PA, USA). DAPI (4′,6-diamidino-2-phenylindole) was supplied by Sigma Chemical Co. (Sigma, Saint Louis, MO, USA), and goat serum was from GIBCO (Invitrogen, Auckland, New Zealand). CitiFluor AF1 antifading mountant was purchased from CitiFluor Ltd. (Leicester, England, U.K.), while DPX mountant (distyrene, plasticizer and xylene) was obtained from BDH Chemicals Ltd. (Poole, England, U.K.). PBS Dulbecco A was supplied by Oxoid Limited (Basingstoke, Hampshire, England, U.K.), and one tablet was dissolved in 100 mL of Milli-Q water (Millipore, Bedford, MA, USA) to obtain a 1× PBS solution.

Corneal Wounding Procedure and Treatment with Cx43 AsODNs. Male Wistar rats (190−220 g) were used throughout the studies, and all experiments were performed with ethics approval from the University of Auckland Animal Ethics Committee (AEC/04/2004/R250). Animals were anesthetized, and corneal laser surgery was mimicked by mechanical scrape wounding performed under a standard laboratory dissecting microscope (Carl Zeiss MicroImaging, Göttingen, Germany). Using a sterile 2 mm diameter dermal biopsy punch (Miltex, York, PA, USA), the central part of the cornea was demarcated and the epithelium within was carefully removed using a scalpel blade (Swann Morton, Sheffield, England) (Figure 2). Bowman's layer, a rigid connective tissue sheet, served as natural scraping

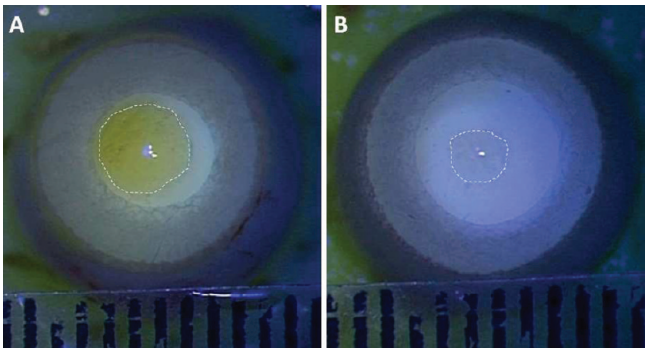

Figure 3. Fluorescein staining showing the wound area of an untreated (A) and a Cx43 AsODN in gellan gum treated (B) eye 12 h after corneal surgery.

basal barrier. All scrape wounding surgeries were performed at the same time of the day to avoid circadian rhythm related inconsistencies in migration and keep proliferation rates to a minimum.[35−37]

For AsODN treatment, 10 μL of each formulation, containing a final Cx43 AsODN concentration of 2 μM, was applied to the wound site of the left eye immediately after surgery using a positive displacement pipet (Finpipette, Labsystems, Helsinki, Finland). Systems without the AsODN incorporated served as controls and were applied to the right eye of the same rat. After predetermined post-treatment times (3, 8, 12, and 24 h), rats were euthanized by carbon dioxide asphyxiation and eyes were enucleated for further analysis.

Penetration Study Using Confocal Laser Scanning Microscopy. Corneal wounding was performed as described above, and formulations containing a final concentration of 2 μM of Cy3 fluorescently tagged AsODNs were applied to the wound site immediately after surgery. Three hours after application, rats were euthanized and eyes were enucleated. Eyes were attached to the bottom of a Petri dish with a drop of superglue, and the Petri dish was filled with PBS. The penetration depth was assessed by performing *z*-scans on a Leica confocal laser scanning microscope (Leica DMRXA 2 microscope fitted with a TCS-SP2 scanhead, Leica Microsystems, Heidelberg, Germany) using a 10× water immersion lens, a zoom of 1 and a pinhole of 2 Airy disk diameter. Optical slices were taken in 20 μm steps over a total range of 600 μm. Three dimensional reconstructions of the *z*-stacks were generated using AMIRA visualizing and analyzing software (Version 3.1, Visage Imaging, San Diego, CA, USA). Penetration depths at the wound site and penetration distances along the epithelium at the wound leading edge were measured using ImageJ (Version 1.41, National Institutes of Health, Bethesda, MD, USA).

Macroscopic Appearance of the Wound Area Using Fluorescein Staining. Corneal wounding and treatment with Cx43 AsODNs were performed as described above. Eyes were enucleated 12 h after application of the formulations, and two drops of concentrated fluorescein solution (Fluorescein paper, Haag-Streit International, Köniz, Switzerland) were dropped onto the corneal surface to visualize the remaining wound area with fluorescein adhering to the corneal stroma in places where the epithelium had been removed.[38] Images were recorded with a Panasonic camera mounted onto a Takagi OM-5 dissection microscope (Takagi Seiko Co. Ltd., Nagano-Ken, Japan), and wound areas were measured in ImageJ using a ruler as calibration scale (Figure 3).

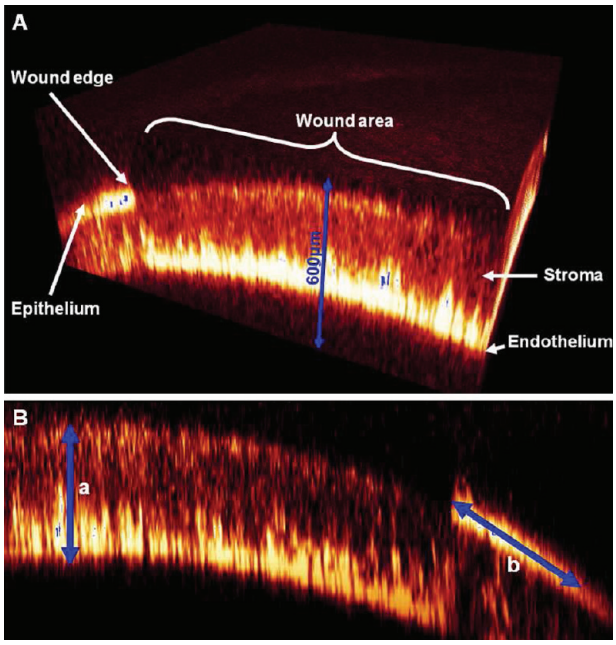

Figure 4. (A) Three dimensional reconstruction of optical slices obtained by confocal laser scanning microscopy showing the penetration depth of the fluorescently tagged Cx43 AsODNs into the corneal tissues. (B) Frontal view of a *z*-stack illustrating the penetration depths measurements of the Cy3-tagged Cx43 AsODNs at the wound site (a) and along the epithelium adjacent to the wound leading edge (b).

Tissue Collection and Processing. Enucleated eyes were rinsed in PBS, embedded in Tissue-Tek OCT and frozen in liquid nitrogen. Frozen tissue blocks were stored at −80 °C until further processed. Sections (16 μm) were cut parallel to the optical axis of the eye using a Zeiss Microm HM550 cryostat (Carl Zeiss NZ. Ltd., Auckland, New Zealand) and were placed on Superfrost Plus slides.

Histology Documentation of the Corneal Wound Healing Dynamics. Hematoxylin and Eosin (H&E) staining was performed according to Mayer. Sections were mounted with DPX mounting medium and viewed under the light microscope (Leica DMRA, Leica Microsystems, Heidelberg, Germany) the following day. Images were recorded with a digital camera (Nikon Digital Sight DS-U1) and the NIS-Elements BR imaging software (Version 2.10). The histology of controls and AsODN treated corneas was compared in terms of stromal thickness and number of cells infiltrating the stroma.

Immunolabeling of Cx43 Protein Channels. Slides were washed twice in PBS for 5 min to remove excess Tissue-Tek. Nonspecific antibody binding was blocked by 10% normal goat serum in PBS for 1 h. Sections were incubated with the monoclonal rabbit anti-Cx43 primary antibody (dilution 1:1000 in PBS) at 4 °C overnight. After the slides were rinsed in PBS three times for 15 min, sections were incubated with a Cy3-conjugated goat anti-rabbit IgG secondary antibody (dilution 1:400 in PBS) for 2 h at room temperature. Sections were again washed in PBS three times for 10 min, before counterstaining cell nuclei with DAPI for 10 min (dilution 1:10 in PBS). After washing the slides another three times, sections were mounted in Citifluor. Slides were viewed under a Zeiss confocal laser scanning microscope (Zeiss Axioplan 2 microscope fitted with a LSM 510 Meta scanhead, Carl Zeiss MicroImaging, Göttingen, Germany).

DAPI-staining and Cx43-labeling were imaged simultaneously by UV light and a 543 nm HeNe laser using the Zeiss LSM 510 Meta software. Single optical slices close to the wound leading edge were taken using a 20× dry objective lens, and the Cx43 expression levels in the controls and the AsODN treated corneas were compared.

RESULTS

Penetration Study Using Confocal Laser Scanning Microscopy. Figure 4A illustrates a 3D-reconstruction of the *z*-stacks obtained by confocal laser scanning microscopy and visualized by AMIRA software. Cy3-tagged AsODNs penetrated freely through the hydrophilic stroma in the wound area where the epithelium had been removed. Further penetration into the anterior chamber was prevented by Descemet's membrane and the endothelium which formed a barrier to the highly hydrophilic AsODNs. In areas where the epithelium was still intact, very little Cy3-tagged AsODN was detectable in the stroma beneath, although large quantities accumulated in the epithelium close to the wound leading edge.

Using a 10× water immersion lens only a quarter to a third of the rat eye could be monitored at once. However, this was sufficient to determine the penetration depth in the central cornea (Figure 4B(a)) and the penetration distance centrifugally along the epithelium adjacent to the wound leading edge (Figure 4B(b)). Table 1 summarizes the penetration depths of the Cy3-tagged AsODNs incorporated into the various formulations. Stromal penetration depths at the wound site ranged from 330 to 370 μm, and the AsODN was also found to accumulate in the epithelium up to 380 μm away from the wound edge.

Table 1. Penetration Depths of the Cy3-Tagged AsODNs Delivered by the Various Formulations at the Wound Site and along the Epithelium Adjacent to the Wound Edge[a]

	penetration ± SD (μm)	
formulation	depth at wound site	distance along epithelium adjacent to wound edge
gellan gum	349.8 ± 14.6	339.3 ± 43.0
carrageenan	366.7 ± 10.2	335.6 ± 26.7
HPMC	355.3 ± 5.5	353.7 ± 31.2
chitosan	354.8 ± 15.1	339.3 ± 43.0
PBS	330.1 ± 9.8	302.3 ± 27.9

[a] Results represent mean values ± SD, $n = 3$.

Macroscopic Appearance of the Wound Area Using Fluorescein Staining. Figure 5 illustrates the initial wound size as well as the wound areas of untreated, control vehicle and Cx43 AsODN treated eyes 12 h after surgery. Measurements of the initial wound size were included to prove the reproducibility of the mechanical scrape wounds and to demonstrate the applicability of the fluorescein staining method to analyze the wound area. The wound area, which was obtained using a 2 mm diameter dermal biopsy punch, was slightly bigger ($A_{experimental}$ = 3.26 ± 0.06 mm^2) than the theoretically calculated value ($A_{theoretical} = \pi r^2$ = 3.14 mm^2), but exhibited only minor discrepancies between eyes (±1.88%). When comparing corneas treated with the different formulations 12 h after surgery, all AsODN treated eyes, with exception of the chitosan treatment group, exhibited a reduction in wound size compared to application of the vehicle alone.

A two-way ANOVA was performed, and no significant difference ($P > 0.05$) was detected between the six rats in each treatment group, confirming the reproducibility of the mechanical scrape wounding model and the associated healing process. Conducting a paired *t*-test on each formulation at a 95% confidence interval, wound areas of the eyes treated with the AsODN incorporated into the gellan gum and carrageenan formulations were found to be significantly different (P = 0.016 and P = 0.048 respectively) from the control eyes of the same treatment group. However, despite the relatively small wound areas of the AsODN treated eyes in the HPMC group, these were not significantly different (P = 0.19) from those treated with HPMC vehicle alone. All chitosan treated eyes exhibited wound areas greater than 2 mm^2 12 h after scrape

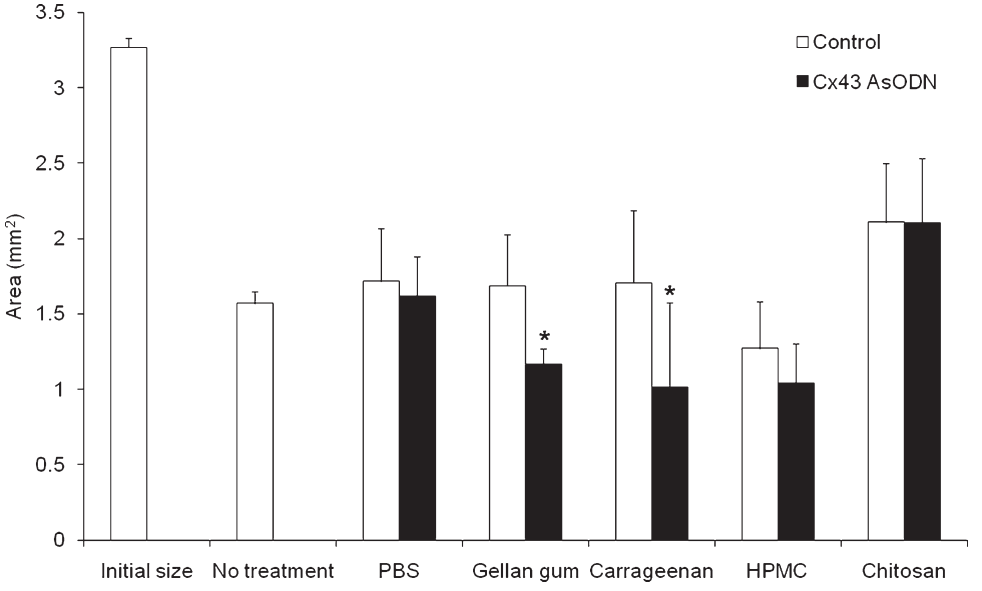

Figure 5. Wound areas of untreated, control and Cx43 AsODN treated eyes for the various delivery vehicles 12 h after mechanical scrape wounding (results represent mean values + SD, $n = 6$, *$P < 0.05$).

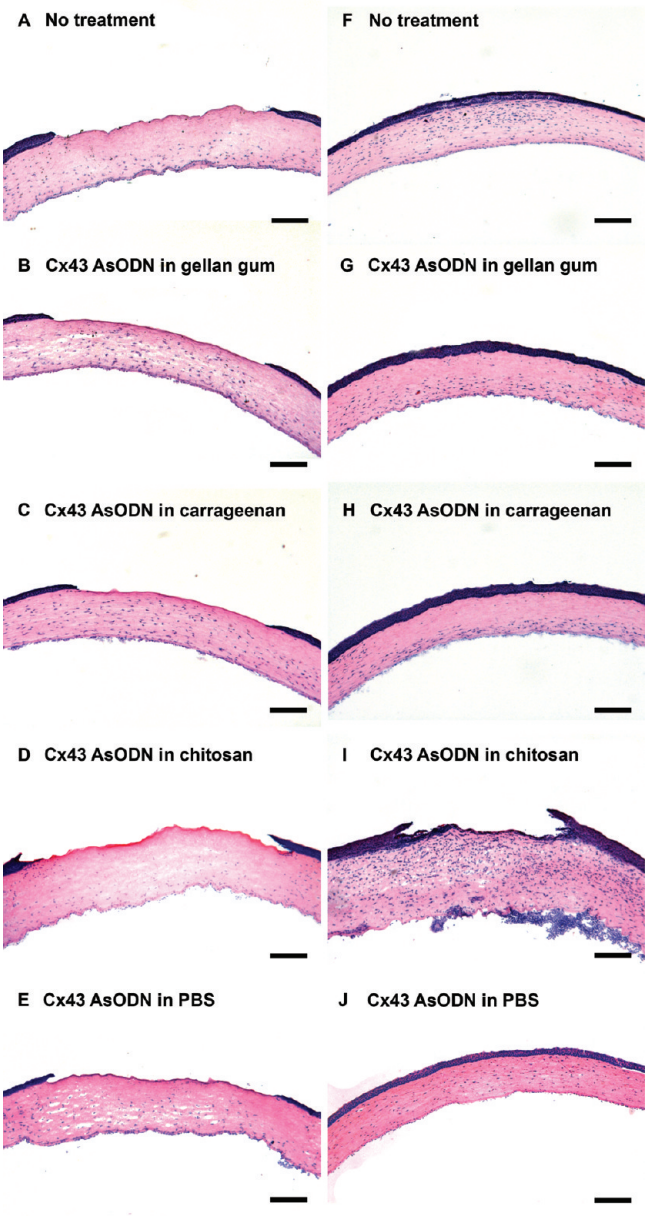

Figure 6. Histological documentation of the corneal healing dynamics 12 h (left column, A−E) and 24 h (right column, F−J) after scrape wounding; scale bar = 200 μm. For clarification of the constituent layers of the cornea refer to Figure 7.

wounding and showed no size difference between control and Cx43 AsODN treated wounds.

Histology Documentation of the Corneal Wound Healing Dynamics. Histology revealed a stromal thickness of about 250 μm for unwounded corneas with evenly spaced keratocytes within the stroma (image not shown). Following wounding, the stromal thickness was increased in all cases, although less pronounced in corneas treated with Cx43 AsODNs compared to controls. Keratocyte loss was most apparent 8 h postwounding in the stroma beneath the wound area of all control corneas. Keratocytes were still absent in the stroma underlying the wound site of the untreated cornea 12 h after surgery (Figure 6A), while corneas treated with the AsODN incorporated into the gellan gum and carrageenan formulations exhibited an almost normal

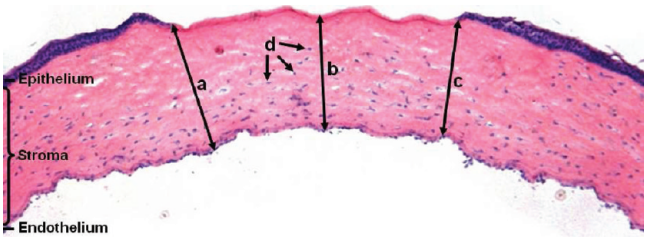

Figure 7. Light microscope image of an H&E-stained cornea illustrating how stromal thickness (a−c) and number of cells within the stroma underlying the wound (d) were determined.

cell distribution in the stroma (Figure 6B,C). These two treatment groups also showed evidence of a new epithelial sheet across the wound bed and the least stromal edema at that time point. In the chitosan and PBS vehicle groups, AsODN treated corneas (Figure 6D,E) revealed keratocyte loss in the stroma underlying the wound as well as stromal edema.

At 24 h after corneal surgery (Figure 6, right column), all wounds apart from the cornea treated with the chitosan formulation (Figure 6I) were closed. However, substantial differences were seen in the extent of stromal edema and hypercellularity. While the untreated cornea, demonstrating normal wound healing dynamics, showed an invasion of ovoid and elongated cells into the anterior part of the stroma underlying the initial wound site, corneas treated with the AsODN incorporated into the gellan gum and carrageenan formulations (Figure 6G,H) lacked cells in this area. The latter two also exhibited a noticeable reduction in corneal thickness when compared to the untreated control, which showed signs of edema, characterized by empty spaces and swelling in the tissue. The epithelium of the chitosan formulation treated corneas did not heal within the 24 h period assessed, and a massive inflammatory response was seen as infiltration of large numbers of round cells into the stroma (Figure 6I). In addition, the stroma was almost double the thickness of the other corneas at 24 h and showed severe signs of edema. This suggests a toxic effect of the positively charged chitosan on the wounded tissues, as had already been apparent when comparing the wound areas at 12 h (Figure 5).

To quantify delivery efficacy and potential toxicity of the formulations, histology images were analyzed in terms of the mean stromal thickness in the wound area (Figure 7a−c) and the number of cells infiltrating the stroma underlying the wound (Figure 7d) 8 and 12 h after corneal surgery using ImageJ. Image analysis results are summarized in Figure 8 and illustrate that all Cx43 AsODN treated corneas irrespective of the time point assessed or the delivery system used showed improved healing characteristics, except for the number of cells at 8 h using the chitosan formulation. The most pronounced effects were seen using gellan gum and carrageenan as delivery vehicles, resulting in the smallest wounds, the least stromal edema and the lowest number of cells infiltrating the stroma. The chitosan formulation, on the other hand, exhibited the highest values for all these parameters with a very large number of inflammatory cells within the stroma at 8 and 12 h postsurgery. This was also apparent in Figure 6I and resulted in delayed wound closure.

Immunolabeling of Cx43 Protein Channels. To determine whether differences in healing rates and Cx43 specific AsODN delivery correlated with changes in Cx43 gap junction levels, immunohistochemistry labeling of Cx43 was carried out. Figure 9 shows Cx43 protein expression levels in an unwounded cornea

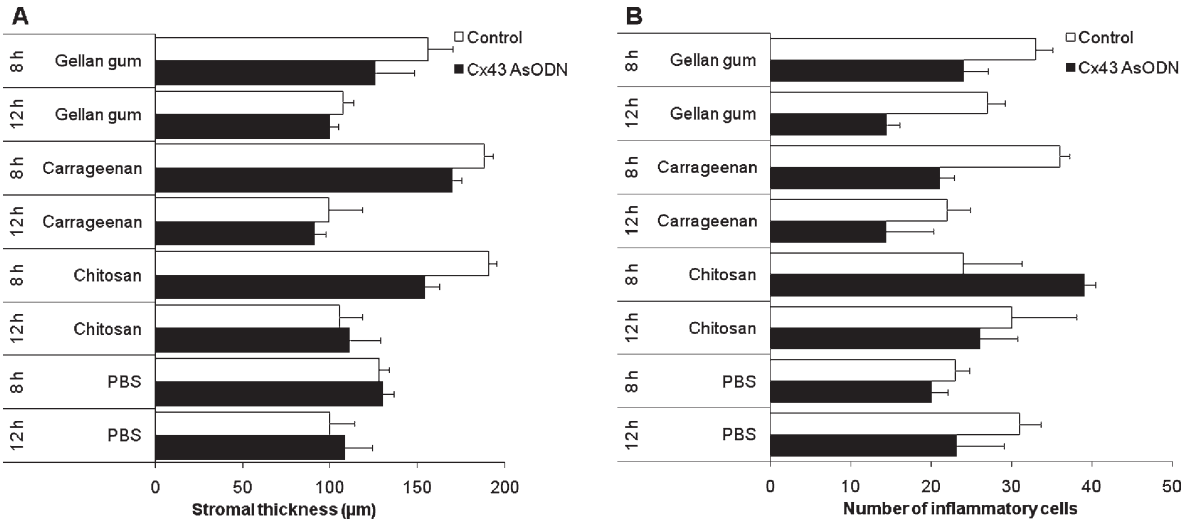

Figure 8. Mean stromal thickness in the wound area (A) and number of cells within the stroma underlying the wound (B) 8 and 12 h postsurgery following application of formulations with and without Cx43 AsODNs (data points represent mean values + SD).

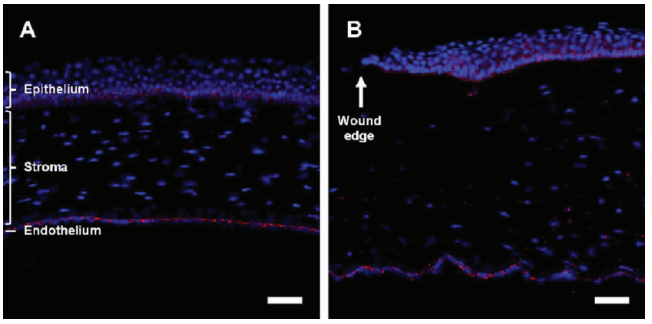

Figure 9. Cx43 protein expression in an unwounded cornea (A) and an untreated wounded cornea (B) 12 h after surgery. Each photomicrograph represents a combined image of Cx43 (red) and DAPI (blue) staining. Scale bar = 50 μm. DAPI staining revealed even distribution of keratocytes in the stroma of the unwounded cornea and confirmed Cx43 expression in the basal cell layer of the epithelium, between keratocytes in the stroma and in the endothelium. Keratocytes were absent in the anterior stroma of the wounded cornea and the tissue showed signs of hyperplasia, which correlated with increased Cx43 expression in the upper layers of the epithelium.

(Figure 9A) and an untreated wounded cornea 12 h after corneal surgery (Figure 9B). DAPI staining revealed an even distribution of keratocytes in the stroma of the unwounded cornea. Cx43 expression was restricted to the basal cell layer of the corneal epithelium and was also found between keratocytes in the stroma and in the endothelium. The wounded cornea exhibited signs of stromal edema and an upregulation of Cx43 levels into the upper layers of the epithelium adjacent to the wound leading edge.

In corneas treated with vehicles alone or formulations containing AsODNs, Cx43 was absent in the stroma underlying the wound area at 8 h postwounding, correlating with the disappearance of cell nuclei as recorded by DAPI counterstaining. Keratocyte loss, however, seemed to be less pronounced in AsODN treated corneas, which also exhibited reduced hypercellularity in the posterior stroma as well as reduced stromal swelling. Cx43 expression was reduced in all wounded corneal epithelia at the wound edge but was even more pronounced in AsODN treated corneas (apart from the cornea using chitosan as delivery vehicle), with Cx43 absent at the immediate wound leading edges and migration of new epithelial cells across the wound bed evident. No difference was seen in Cx43 levels of the chitosan treatment group, where Cx43 expression appeared to be extended to the intermediate cells of the epithelium, correlating with signs of hyperplasia and delayed wound closure.

At 12 h after corneal surgery (Figure 10), keratocytes were still absent from the anterior stroma of all corneas. However, control vehicle corneas (Figure 10A,C,E,G) and the chitosan treated cornea (Figure 10F) exhibited increased infiltration of cells in the posterior stroma and at the wound periphery as seen by DAPI staining. These corneas also showed signs of hyperplasia, which correlated with increased Cx43 expression levels in the upper layers of the epithelium. In the AsODN treated corneas using gellan gum and carrageenan as delivery vehicle, Cx43 expression was significantly reduced and was found to be absent in the wound leading edges where new epithelial cells were seen to be migrating across the wound bed. These corneas also showed a noticeable reduction in stromal edema compared to the control corneas, although stromal thickness was still slightly increased compared to the prewounding situation (Figure 9A).

All wounds, apart from those in the chitosan treatment group, were closed 24 h after surgery. Cx43 protein levels still appeared slightly overexpressed, but were relocated to the basal cell layers of the epithelium, apart from the area where the migrating epithelial sheets from either side had come together and slight signs of overexpression, correlating with hyperplasia, were detected.

DISCUSSION

The actual size of the wounds initially generated was slightly bigger than the theoretically calculated value of 3.14 mm^2, but revealed only minor discrepancies between eyes ($\pm$1.88%). Moreover, a two-way ANOVA performed on the results for the wound areas after 12 h showed no significant difference ($P > 0.05$) between the six rats in each treatment group, confirming the reproducibility of the mechanical scrape wounding model and the associated healing response. It is possible that excimer laser photorefractive keratectomy would result in more

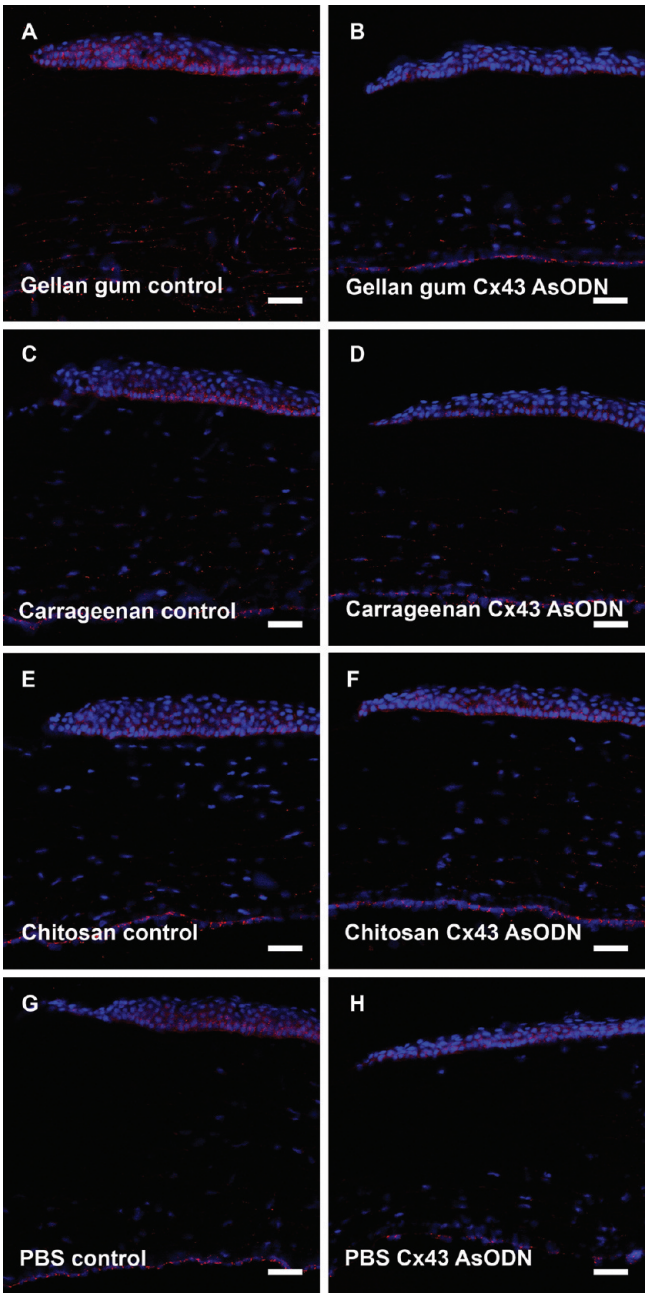

Figure 10. Cx43 protein expression in control and Cx43 AsODN treated corneas 12 h after surgery. Each photomicrograph represents a combined image of Cx43 (red) and DAPI (blue) staining, resulting from a single optical confocal slice. Scale bar = 50 μm. Keratocytes were still absent in the anterior stroma of all corneas, but control corneas exhibited increased infiltration of cells in the posterior stroma and further from the wound leading edge. They also showed signs of hyperplasia, which correlated with increased Cx43 expression in the upper layers of the epithelium. In the AsODN treated corneas of the gellan gum and carrageenan treatment group, Cx43 expression was significantly reduced and absent at the wound leading edge and in the stroma, which also exhibited less swelling compared to the controls. Moreover, epithelial cells were seen to be migrating across the wound bed in the AsODN treated corneas.

reproducible wounds, although the clear wound healing response in the scrape wounding model makes differences in delivery efficacy easy to monitor.

For this study, no treatment (reflecting normal corneal wound healing) and application of the vehicle alone were used as control experiments, as the primary aim was to investigate the formulation effect. In order to evaluate the efficacy of the various formulations to successfully deliver Cx43 AsODNs to the wounded tissue, a number of studies were performed. First, confocal laser scanning microscopy was used to evaluate whether the AsODN was able to penetrate into the corneal tissues, and to where. AsODNs freely penetrated through the hydrophilic stroma at the wound site, but were prevented from further penetration into the ocular tissues by Descemet's membrane and the lipophilic endothelium. In areas where the epithelium was still intact, only small amounts of Cy3-labeled AsODN were detected in the epithelium and the underlying stroma, indicating that the highly hydrophilic AsODNs have difficulty passing an intact epithelial surface. The observation that most of the AsODN seemed to accumulate at the wound leading edges of the epithelium was favorable as this results in Cx43 protein knockdown predominantly in these areas. The *in situ* gelling systems tested here were suitable for delivery of hydrophilic molecules where the epithelium had been removed, but may be less appropriate where the corneal epithelium is intact.

The second method used to differentiate delivery system efficacy was measurement of the wound areas 12 h after surgery using fluorescein staining. The improvement in the wound healing response was found to be significantly different ($P < 0.05$) when the Cx43 AsODN was delivered using the gellan gum and carrageenan systems. This could be attributed to the ability of these polymers to cross-link with the cations present in the tear fluid, resulting in increased viscosity and therefore reduced lacrimal drainage of the drug as previously discussed.[33,34] This would result in an overall increased bioavailability of the Cx43 AsODNs and therefore an improved healing response as confirmed by histological analysis.

The difference between HPMC vehicle alone and HPMC with AsODNs was not significant, although the wound sizes of the AsODN treated corneas in the HPMC group were comparable to those of the carrageenan group. HPMC alone appeared to have a positive effect on wound healing, as even those wounds receiving the vehicle only exhibited noticeably smaller wound areas. This may be associated with the lack of charge in the polymer backbone as opposed to the anionic and cationic nature of the other polymers used, therefore resulting in less interaction with other cellular components, as well as the wound hydration effect of HPMC. For this study the HPMC formulation was excluded from subsequent experiments, as it would not have been possible to differentiate between the vehicle only and the Cx43 AsODN effect. However, this observation warrants further investigation.

Chitosan, on the other hand, had a negative effect on the wound healing rate, as both the control and the Cx43 AsODN treated corneas still showed wound areas greater than 2 mm^2 at 12 h postsurgery. The lack of difference between control and AsODN treated corneas in this group could be attributed to the precipitation of the AsODN out of solution. This observation was made during the penetration studies where fluorescently tagged AsODNs, incorporated into the chitosan system, were found at least partially precipitated out of solution. The negative effect of the chitosan formulation itself was even more obvious when evaluating histology and Cx43 levels. While most corneas treated with control formulations exhibited cellular responses comparable to untreated eyes, chitosan treated control corneas showed a pronounced inflammatory response.

A number of research groups have reported chitosan to be a wound-healing accelerator.[39,40] However, views on wound healing have changed markedly over the past few years. While a proinflammatory response was previously considered to be beneficial, recent investigations support the paradigm that increased inflammation has a negative effect on the rate of wound closure and increases subsequent scarring.[41] Several studies performed on the skin[11,42] and the eye[43] have shown that a decrease in the inflammatory response, due to depletion in neutrophil numbers, resulted in an accelerated wound closure. Although neutrophils may initially provide protection against infection, they also delay wound closure and cause additional tissue damage. The increased invasion of inflammatory cells in the chitosan group, which has previously been claimed to accelerate wound healing, was here found to have the opposite effect. This was shown by severe swelling of the corneal tissue, with the stromal thickness measuring approximately double the thickness compared to other corneas. Moreover, chitosan treated wounds were still open 24 h after surgery, while all other corneas exhibited a completely healed epithelium.

For the other delivery vehicles, H&E staining revealed an increase in stromal swelling for all corneas at the time points monitored. However, stromal edema was less pronounced in AsODN treated corneas, especially when gellan gum and carrageenan were used as delivery vehicles. These corneas also showed less infiltration of inflammatory cells and greater evidence of new epithelial cell sheets sliding across the wound bed. This may again be attributed to the *in situ* gelling nature of these formulations, forming a gel on the ocular surface once in contact with the cations in the tear fluid to prolong precorneal retention. This would allow for sustained delivery, resulting in improved healing dynamics.

These findings were further supported by results obtained from Cx43 immunoassays. While all corneas showed a slight reduction in Cx43 levels 8 h after surgery, this effect was even more pronounced in the gellan gum and carrageenan AsODN treated corneas where Cx43 was found to be completely absent at the wound leading edges. Reduction in intercellular communication at the wound leading edges is desirable after surgery to promote epithelial cell migration.[11] However, gap junctional communication back from the wound edge is required in order to promote proliferation of epithelial cells for wound closure.

At 12 h after corneal surgery, Cx43 expression in the control groups had extended to the upper layers of the epithelium, correlating with signs of hyperplasia. This was in agreement with previous studies performed by Ratkay-Traub et al.,[18] who found Cx43 to be upregulated adjacent to the wound edges and not restricted to the basal epithelial cells. When comparing control to AsODN treated corneas, extension of Cx43 protein expression to the upper cell layers of the epithelium was not seen, apart from the area where the migrating epithelial sheets from either side had come together to close the wound. Finally, the extent of stromal edema was reduced and the anterior stroma of the AsODN treated corneas using gellan gum and carrageenan as delivery vehicle showed no signs of inflammatory cell infiltration, supporting the assumption that ion-activated *in situ* gelling systems based on these two polymers improve the delivery of Cx43 AsODNs to the corneal tissues when compared to a chitosan system or a saline solution.

CONCLUSION

Penetration studies emphasized that delivery occurred mainly to the epithelium at the wound leading edges and the stroma underlying the wound, therefore preventing lesion spread but allowing for cell proliferation in the periphery of the cornea. Control experiments using the vehicle alone revealed potential toxicity of the positively charged chitosan polymer backbone, while uncharged HPMC seemed to promote a positive wound healing response. In all studies performed, Cx43 AsODN formulations based on gellan gum and carrageenan exhibited the best results in terms of remaining wound size, reduction in inflammatory response and reduced Cx43 protein levels. This is mainly attributed to the *in situ* gelling effect of these systems once in contact with the cations of the tear fluid and therefore increased precorneal retention time. It would appear that delivery systems based on gellan gum and carrageenan are able to retain AsODNs on the corneal surface without inducing any evidence for adverse effects.

AUTHOR INFORMATION

Corresponding Author

*Department of Ophthalmology, Faculty of Medical and Health Sciences, The University of Auckland, Private Bag 92019, Auckland, New Zealand. Phone: +64 9 923 6386. Fax: +64 9 367 7173. E-mail: i.rupenthal@auckland.ac.nz.

ACKNOWLEDGMENT

The authors would like to thank Silke Fuchs for her skilled assistance with the tissue cutting and H&E staining procedures and Marian Kelly, Sonalee Ghosal, Debby Chen, Hwiju Park and Tzu-Hong Chang for their support with the histological picture analysis. Thanks also to the University of Auckland for the financial support in the form of an international doctoral scholarship for I.D.R. and CP Kelco for kindly donating samples of gellan gum and carrageenan polymers.

ABBREVIATIONS USED

Cx43, connexin43; AsODN(s), antisense oligodeoxynucleotide(s); HPMC, hydroxypropyl methylcellulose; PBS, phosphate buffered saline; H&E, Hematoxylin and Eosin

REFERENCES

(1) Netto, M. V.; Mohan, R. R.; Ambrosio, R., Jr.; Hutcheon, A. E.; Zieske, J. D.; Wilson, S. E. Wound healing in the cornea: a review of refractive surgery complications and new prospects for therapy. *Cornea* **2005**, *24* (5), 509–22.

(2) Wilson, S.; Mohan, R.; Hong, J.; Lee, J. The wound healing response after laser in situ keratomileusis and photorefractive keratectomy: elusive control of biological variability and effect on custom laser vision correction. *Arch. Ophthalmol.* **2001**, *119* (6), 889–896.

(3) Wilson, S. E.; Mohan, R. R.; Mohan, R. R.; Ambrosio, R.; Hong, J.; Lee, J. The Corneal Wound Healing Response: Cytokine-mediated Interaction of the Epithelium, Stroma, and Inflammatory Cells. *Prog. Retinal Eye Res.* **2001**, *20* (5), 625–637.

(4) Cordeiro, M. F.; Mead, A.; Ali, R. R.; Alexander, R. A.; Murray, S.; Chen, C.; York-Defalco, C.; Dean, N. M.; Schultz, G. S.; Khaw, P. T. Novel antisense oligonucleotides targeting TGF-beta inhibit in vivo scarring and improve surgical outcome. *Gene Ther.* **2003**, *10* (1), 59–71.

(5) Kaur, H.; Chaurasia, S. S.; de Medeiros, F. W.; Agrawal, V.; Salomao, M. Q.; Singh, N.; Ambati, B. K.; Wilson, S. E. Corneal stroma

PDGF blockade and myofibroblast development. *Exp. Eye Res.* **2009**, *88* (5), 960–965.

(6) Evans, W. H.; Martin, P. E. Gap junctions: structure and function. *Mol. Membr. Biol.* **2002**, *19* (2), 121–36.

(7) Fallon, R. F.; Goodenough, D. A. Five-hour half-life of mouse liver gap-junction protein. *J. Cell Biol.* **1981**, *90* (2), 521–6.

(8) Kumar, N. M.; Gilula, N. B. The gap junction communication channel. *Cell* **1996**, *84* (3), 381–8.

(9) Spray, D. C. Molecular physiology of gap junction channels. *Clin. Exp. Pharmacol. Physiol.* **1996**, *23* (12), 1038–40.

(10) Laux-Fenton, W. The role of connexins in corneal homeostasis and repair: mastering the connections to improve repair. Thesis (PhD), The University of Auckland, Auckland, New Zealand, 2003.

(11) Qiu, C.; Coutinho, P.; Frank, S.; Franke, S.; Law, L.-y.; Martin, P.; Green, C. R.; Becker, D. L. Targeting Connexin43 Expression Accelerates the Rate of Wound Repair. *Curr. Biol.* **2003**, *13* (19), 1697–1703.

(12) Coutinho, P.; Qiu, C.; Frank, S.; Wang, C. M.; Brown, T.; Green, C. R.; Becker, D. L. Limiting burn extension by transient inhibition of Connexin43 expression at the site of injury. *Br. J. Plast. Surg.* **2005**, *58* (5), 658–667.

(13) Wang, C. M.; Lincoln, J.; Cook, J. E.; Becker, D. L. Abnormal connexin expression underlies delayed wound healing in diabetic skin. *Diabetes* **2007**, *56* (11), 2809–17.

(14) Gourdie, R. G.; Ghatnekar, G. S.; O'Quinn, M.; Rhett, M. J.; Barker, R. J.; Zhu, C.; Jourdan, J.; Hunter, A. W. The unstoppable connexin43 carboxyl-terminus: new roles in gap junction organization and wound healing. *Ann. N.Y. Acad. Sci.* **2006**, *1080*, 49–62.

(15) Chanson, M.; Derouette, J. P.; Roth, I.; Foglia, B.; Scerri, I.; Dudez, T.; Kwak, B. R. Gap junctional communication in tissue inflammation and repair. *Biochim. Biophys. Acta* **2005**, *1711* (2), 197–207.

(16) Beyer, E. C.; Kistler, J.; Paul, D. L.; Goodenough, D. A. Antisera directed against connexin43 peptides react with a 43-kD protein localized to gap junctions in myocardium and other tissues. *J. Cell Biol.* **1989**, *108* (2), 595–605.

(17) Dong, Y.; Roos, M.; Gruijters, T.; Donaldson, P.; Bullivant, S.; Beyer, E.; Kistler, J. Differential expression of two gap junction proteins in corneal epithelium. *Eur. J. Cell Biol.* **1994**, *64* (1), 95–100.

(18) Ratkay-Traub, I.; Hopp, B.; Bor, Z.; Dux, L.; Becker, D. L.; Krenacs, T. Regeneration of rabbit cornea following excimer laser photorefractive keratectomy: a study on gap junctions, epithelial junctions and epidermal growth factor receptor expression in correlation with cell proliferation. *Exp. Eye Res.* **2001**, *73* (3), 291–302.

(19) Gabbiani, G.; Chaponnier, C.; Huttner, I. Cytoplasmic filaments and gap junctions in epithelial cells and myofibroblasts during wound healing. *J. Cell Biol.* **1978**, *76* (3), 561–8.

(20) Jester, J. V.; Petroll, W. M.; Barry, P. A.; Cavanagh, H. D. Temporal, 3-dimensional, cellular anatomy of corneal wound tissue. *J. Anat.* **1995**, *186* (2), 301–11.

(21) Petridou, S.; Masur, S. K. Immunodetection of connexins and cadherins in corneal fibroblasts and myofibroblasts. *Invest. Ophthalmol. Visual Sci.* **1996**, *37* (9), 1740–8.

(22) Jester, J. V.; Petroll, W. M.; Cavanagh, H. D. Corneal stromal wound healing in refractive surgery: the role of myofibroblasts. *Prog. Retinal Eye Res.* **1999**, *18* (3), 311–356.

(23) Piatigorsky, J. Review: A case for corneal crystallins. *J. Ocul. Pharmacol. Ther.* **2000**, *16* (2), 173–80.

(24) Akhtar, S.; Kole, R.; Juliano, R. L. Stability of antisense DNA oligodeoxynucleotide analogs in cellular extracts and sera. *Life Sci.* **1991**, *49* (24), 1793–801.

(25) Wickstrom, E. Oligodeoxynucleotide stability in subcellular extracts and culture media. *J. Biochem. Biophys. Methods* **1986**, *13* (2), 97–102.

(26) Balasubramaniam, J.; Kant, S.; Pandit, J. K. In vitro and in vivo evaluation of the Gelrite gellan gum-based ocular delivery system for indomethacin. *Acta Pharm.* **2003**, *53* (4), 251–61.

(27) Shedden, A. H.; Laurence, J.; Barrish, A.; Olah, T. V. Plasma timolol concentrations of timolol maleate: timolol gel-forming solution (TIMOPTIC-XE) once daily versus timolol maleate ophthalmic solution twice daily. *Doc. Ophthalmol.* **2001**, *103* (1), 73–9.

(28) Balasubramaniam, J.; Pandit, J. K. Ion-activated in situ gelling systems for sustained ophthalmic delivery of ciprofloxacin hydrochloride. *Drug Delivery* **2003**, *10* (3), 185–191.

(29) Hartmann, V.; Keipert, S. Influence of divalent cations on deacetylated gellan and pilocarpine containing ophthalmic preparations. *Pharm. Pharmacol. Lett.* **1996**, *6* (3), 98–101.

(30) Sultana, Y.; Aqil, M.; Ali, A. Ion-Activated, Gelrite®-Based in Situ Ophthalmic Gels of Pefloxacin Mesylate: Comparison with Conventional Eye Drops. *Drug Delivery* **2006**, *13* (3), 215–219.

(31) Kalam, M. A.; Sultana, Y.; Samad, A.; Ali, A.; Aqil, M.; Sharma, M.; Mishra, A. K. Gelrite-Based In Vitro Gelation Ophthalmic Drug Delivery System of Gatifloxacin. *J. Dispersion Sci. Technol.* **2008**, *29* (1), 89–96.

(32) Greaves, J. L.; Wilson, C. G.; Rozier, A.; Grove, J.; Plazonnet, B. Scintigraphic assessment of an ophthalmic gelling vehicle in man and rabbit. *Curr. Eye Res.* **1990**, *9* (5), 415–20.

(33) Rupenthal, I. D.; Green, C. R.; Alany, R. G. Comparison of ion-activated in situ gelling systems for ocular drug delivery. Part 1: Physicochemical characterisation and in vitro release. *Int. J. Pharm.* **2011**, *411* (1−2), 69–77.

(34) Rupenthal, I. D.; Green, C. R.; Alany, R. G. Comparison of ion-activated in situ gelling systems for ocular drug delivery. Part 2: Precorneal retention and in vivo pharmacodynamic study. *Int. J. Pharm.* **2011**, *411* (1−2), 78–85.

(35) Burns, E. R.; Scheving, L. E. Circadian influence on the wave form of the frequency of labeled mitoses in mouse corneal epithelium. *Cell Tissue Kinet.* **1975**, *8* (1), 61–6.

(36) Lavker, R. M.; Dong, G.; Cheng, S. Z.; Kudoh, K.; Cotsarelis, G.; Sun, T. T. Relative proliferative rates of limbal and corneal epithelia. Implications of corneal epithelial migration, circadian rhythm, and suprabasally located DNA-synthesizing keratinocytes. *Invest. Ophthalmol. Visual Sci.* **1991**, *32* (6), 1864–75.

(37) Scheving, L. E.; Pauly, J. E. Circadian phase relationships of thymidine-3H uptake, labeled nuclei, grain counts, and cell division rate in rat corneal epithelium. *J. Cell Biol.* **1967**, *32* (3), 677–83.

(38) Lebensohn, J. E. Fluorescein in ophthalmology. *Am. J. Ophthalmol.* **1969**, *67* (2), 272–4.

(39) Ueno, H.; Mori, T.; Fujinaga, T. Topical formulations and wound healing applications of chitosan. *Adv. Drug Delivery Rev.* **2001**, *52* (2), 105–115.

(40) Singla, A. K.; Chawla, M. Chitosan: some pharmaceutical and biological aspects--an update. *J. Pharm. Pharmacol.* **2001**, *53* (8), 1047–67.

(41) Dovi, J. V.; Szpaderska, A. M.; DiPietro, L. A. Neutrophil function in the healing wound: adding insult to injury? *Thromb. Haemostasis* **2004**, *92* (2), 275–80.

(42) Dovi, J. V.; He, L.-K.; DiPietro, L. A. Accelerated wound closure in neutrophil-depleted mice. *J. Leukocyte Biol.* **2003**, *73* (4), 448–55.

(43) Ueno, M.; Lyons, B. L.; Burzenski, L. M.; Gott, B.; Shaffer, D. J.; Roopenian, D. C.; Shultz, L. D. Accelerated wound healing of alkali-burned corneas in MRL mice is associated with a reduced inflammatory signature. *Invest. Ophthalmol. Visual Sci.* **2005**, *46* (11), 4097–106.